

Consistent estimates of ^{56}Ni yields for type Ia supernovae

M. Stritzinger^{1,2}, P. A. Mazzali^{2,3}, J. Sollerman^{1,4}, and S. Benetti⁵

¹ Dark Cosmology Centre, Niels Bohr Institute, University of Copenhagen, Juliane Maries Vej 30, DK-2100 Copenhagen Ø, Denmark
e-mail: max@dark-cosmology.dk

² Max-Planck-Institut für Astrophysik, Karl-Schwarzschild-Str. 1, 85741 Garching bei München, Germany

³ INAF-OATs, Via Tiepolo, 11, 34131 Trieste, Italy
e-mail: mazzali@mpa-garching.mpg.de

⁴ Stockholm Observatory, AlbaNova, Department of Astronomy, 106 91 Stockholm, Sweden
e-mail: jesper@dark-cosmology.dk

⁵ INAF - Osservatorio Astronomico di Padova, vicolo dell'Osservatorio 5, I-35122 Padova, Italy
e-mail: stefano.benetti@oapd.inaf.it

Received – / Accepted –

Abstract

Aims. We present ^{56}Ni mass estimates for seventeen well-observed type Ia supernovae determined by two independent methods.

Methods. Estimates of the ^{56}Ni mass for each type Ia supernova are determined from (1) modeling of the late-time nebular spectrum and (2) through the combination of the peak bolometric luminosity with Arnett's rule. The attractiveness of this approach is that the comparison of estimated ^{56}Ni masses circumvents errors associated with the uncertainty in the adopted values of reddening and distance.

Results. We demonstrate that these two methods provide consistent estimates of the amount of ^{56}Ni synthesized. We also find a strong correlation between the derived ^{56}Ni mass and the absolute B -band magnitude (M_B).

Conclusions. Spectral synthesis can be used as a diagnostic to study the explosion mechanism. By obtaining more nebular spectra the ^{56}Ni - M_B correlation can be calibrated, and be used to investigate any potential systematic effects this relationship may have upon the determination of cosmological parameters, and provide a new manner to estimate extra-galactic distances of nearby type Ia supernovae.

Key words. stars: supernovae: general

1. Introduction

Type Ia supernovae (hereafter SNe Ia) are a vital tool for our understanding of the universe. Due to their high luminosities and remarkable uniformity they are excellent cosmological distance indicators, and allow us to determine the evolution of cosmic expansion (see e.g. Leibundgut 2001, and references therein).

Presently astronomical researchers are witnessing the use of SNe Ia as high precision cosmological probes (see Riess et al. 2004; Astier et al. 2006). To utilize the level of precision achieved from current and future experiments requires the ability to understand and reduce any source of systematic error. The main motivation of this work was to gain an understanding of the relationship between the ^{56}Ni mass and peak absolute magnitude.

To understand the dependence of the absolute brightness upon the ^{56}Ni mass requires knowledge of the progenitor system and explosion mechanism of SNe Ia. Despite considerable efforts on the theoretical side to investigate the explo-

sion physics, our current knowledge of the ignition mechanism and subsequent flame propagation through the progenitor star is still rather rudimentary, and in some instances debatable (Hillebrandt & Niemeyer 2000). From an observational perspective, considerable effort has been put forth by supernova monitoring programs around the world and many excellent data sets have been assembled. With these data it is now possible to conduct detailed investigations into the physical mechanism leading to the observed diversity in the SNe Ia population. Some first steps have been made in this direction, e.g. Cappellaro et al. (1997); Mazzali et al. (1998); Contardo et al. (2000); Mazzali et al. (2001); Suntzeff (2003); Benetti et al. (2005); Stritzinger et al. (2006); Branch et al. (2006).

The amount of ^{56}Ni produced in a SN Ia explosion is a key parameter that can be derived from observations and is important for our understanding of the luminosity decline-rate relation. In this article we demonstrate that the amount of ^{56}Ni computed from modeling the late-time nebular spectrum of a SN Ia is consistent with estimates obtained from the combination of the UltraViolet Optical near-InfraRed (UVOIR) bolometric light curve with Arnett's rule (Arnett 1982). We also find

a strong correlation between the derived ^{56}Ni mass and M_B . As we can now estimate the mass of synthesized ^{56}Ni accurately from fitting the nebular spectrum this method may provide a means to understand possible sources of systematic error that could effect the analysis of data from future high- z SNe Ia surveys.

The structure of this paper is as follows. In Sect. 2 we provide a brief description of the observational data considered in this study. Section 3 describes the two methods used to estimate the ^{56}Ni mass. Section 4 contains the results, and is then followed by a discussion in Sect. 5.

2. Observational data

We have analyzed both published and unpublished photometric and spectroscopic CCD data collected by numerous groups over the past two decades. A large fraction of these observations were obtained by the Asiago group, the Center for Astrophysics group, and most recently by the European Supernova Collaboration. Data have also been taken from a variety of sources in the literature. Two selection criteria were fulfilled by each SN Ia in our sample: each event had to have comprehensive photometric (U) BVR I-band light curves that include maximum light as well as at least one nebular spectrum. This spectrum is required for the spectral fitting method (see Sect. 3.1) while the well-sampled light curves are required to produce a reliable UVOIR light curve (see Sect. 3.2).

We were able to compile nebular spectra and photometric data for seventeen events. Table 1 lists relevant information for each event, which includes the number of nebular spectra, adopted values of reddening and distance moduli, as well as an estimate of the B -band light curve decline rate parameter $\Delta m_{15}(B)$.

3. Methods

In this section we provide a short overview of the two methods used to determine the ^{56}Ni mass for each SN Ia.

3.1. Modeling nebular spectra

Here we will only briefly summarize the spectral analysis method; for a more detailed description see Mazzali et al. (1997, 1998) and Stehle et al. (2005). A forthcoming publication will contain a detailed analysis of each modeled nebular spectra considered here (Mazzali, in preparation). This analysis includes constraints on nuclear abundances, mixing within the ejecta, and limits on the extinction.

The ratio between the explosion energy and the ejected mass in thermonuclear supernovae is larger compared to what is found in core collapse supernovae. As a result the ejecta in a SN Ia becomes transparent to γ rays significantly earlier than in a type II SN. After ~ 150 days past maximum light the spectrum can safely be considered nebular. During the nebular phase the emission spectrum is formed in the dense central regions of the ejecta. It is at this location that the majority of Fe-group elements are located. As the abundance of different

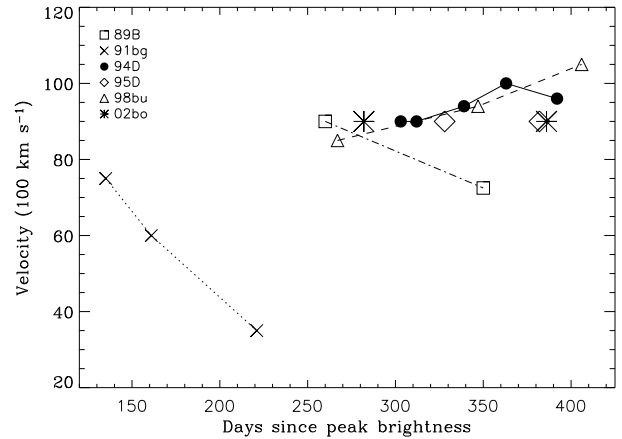


Figure 1 The evolution of the modeled velocity for six SNe Ia as a function of time past maximum brightness.

Fe-group elements is a direct consequence of the nuclear burning process, the modeling of this phase allows for an important opportunity to constrain the explosion mechanism.

Synthetic spectra were calculated for each observed nebular spectrum with a model that uses a non-local thermodynamic equilibrium (NLTE) treatment of the rate equations. The code first computes the deposition of the γ rays and positrons from the radioactive decays using a Monte Carlo approach (Cappellaro et al. 1997). The deposition is transformed into collisional heating following the prescriptions of Axelrod (1980; see also Ruiz-Lapuente & Lucy 1992), and this is then balanced by cooling via line emission. Both forbidden and allowed transitions are included. Forbidden lines dominate the cooling, except for a few ions (Na I, Ca II) where permitted lines dominate. Line emission is computed in concentric shells within which the density and the abundances are constant. Since most lines are blends, we observe the combined effect of density and abundance distribution. The W7 model (Nomoto, Thielemann, & Yokoi 1984) is used throughout for the density distribution. A satisfactory fit with observed line profiles is made by changing the abundances in each shell. Rather than trying to fit the broadest features, which are formed by the blend of many weak lines, we instead fit the two strongest Fe-group features Fe III at 4650 Å and Fe II + Fe III at 5300 Å. This gives a more accurate estimate of the line emissivity and hence of the ^{56}Ni mass.

Based on two infrared nebular spectra Spyromilio et al. (2004) reported evidence for an increase of the expansion velocities as a function of time. We also find an increase in the emission line velocities of SN 1998bu. However, with the total data set considered in this study, which comprises six SNe Ia with at least two spectra (see Table 1), we can not confirm any claim of an increase in line velocities. This is shown in Fig. 1 where we plot the velocity used in the model for the Fe nebula vs. days past maximum brightness. We note that for expansion velocities greater than $\sim 6000 \text{ km s}^{-1}$ the modeled nebular velocity is linearly correlated with the FWHM velocity of the two Fe lines that we fit (see Mazzali et al. 1998).

For all normal SNe Ia we find some dispersion ($\sim 10\%$) about a mean value, however there is no clear trend for any evolution in the line velocities. Only SN 1991bg shows a significant decrease in line velocities. This may be due to the ejecta not having reached the complete nebular phase when the first two spectra were obtained. Moreover, it is known that severe blending of lines occurs between velocities of 3000 to 6000 km s^{-1} making it difficult to obtain a very reliable fit. For events with more than one nebular spectrum we computed the ^{56}Ni mass for each spectrum and then averaged together the estimates.

The main uncertainty affecting our estimate of the ^{56}Ni mass (excluding uncertainties in reddening and distance) comes from the unknown contribution in the infrared (IR), which is known to increase during late-times (Sollerman et al. 2004). Some species, in particular Si, emit only in the IR, and their abundance cannot be constrained directly by modeling the optical spectrum only. However, in the best observed IR spectrum of a SN Ia in the nebular phase (SN 1998bu, Meikle, priv. comm.; Spyromilio et al. 2004) Si emission lines do not make a major contribution. Most of the IR flux is emitted from Fe and Co lines, and much of it is therefore taken into account in our models. We estimate that the error in our estimate of the ^{56}Ni mass including errors associated with our code, the flux contribution in the IR, and possible systematic errors due to uncertain calibration of the late-time spectra, is on the order of $\sim 15\%$ (see below).

3.2. The UVOIR light curve and Arnett's rule

A complete description of how to derive the ^{56}Ni mass using broad-band optical photometry is presented in Contardo et al. (2000). The overall strategy is to construct a quasi-bolometric light curve which allows us to avoid the complicated radiative transfer required to interpret single passband light curves. The early-time UVOIR light curve of a SN Ia is known to include most of the total *true* bolometric flux (Suntzeff 1996; Contardo et al. 2000). At maximum light the UVOIR light curve does not account for the $\sim 5\%$ contribution of flux emitted in the IR nor any flux blue-wards of 3200 \AA . These contributions add up to less than $\sim 15\%$ of the total flux.

Following Contardo et al., the $(U)BVRI$ photometric light curves are fitted with a 10-parameter function. This function contains no physics, rather it produces a continuous description of each light curve and a set of parameters that can be compared to one another. To calculate a UVOIR light curve each filter light curve is summed together and a correction is made to account for the extinction. When U -band data is lacking (see Table 1) a correction based on SN 1992A (Suntzeff 1996) is applied in the manner described by Contardo et al. (2000). Finally, the absolute flux scale is set with an accurate distance¹.

¹ When possible a direct distance measurement, e.g. a Cepheid distance estimate, is adopted. If no direct distance measurement is available we used relative distances to Virgo (Kraan-Korteweg 1986) adopting a Virgo distance of 15.3 Mpc or distances from the Hubble flow.

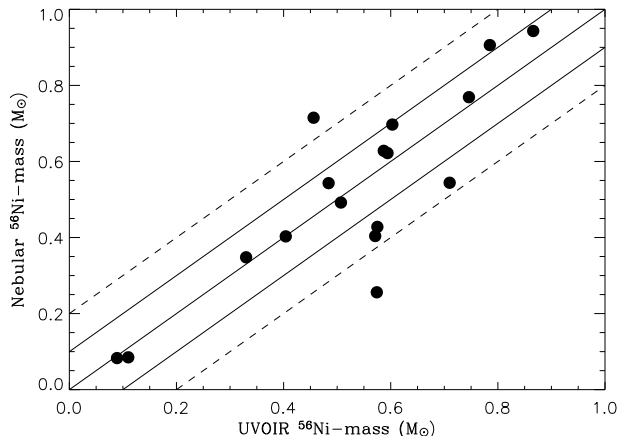


Figure 2 Plot of ^{56}Ni mass derived for seventeen SNe Ia via the late-time nebular spectrum fitting method vs. the UVOIR bolometric light curve method. Dashed and dotted slanted lines correspond to 10% and 20% offsets from the slope of the solid line, respectively.

To derive the ^{56}Ni mass we make use of Arnett's rule (Arnett 1982), which states that at the time of maximum light the SN Ia luminosity is equal to the energy inputs from the radioactive decays within the expanding ejecta. A derivation of an empirical relation for Arnett's rule that connects the observed luminosity at maximum light to the ^{56}Ni mass is given in Stritzinger & Leibundgut (2005). Assuming a rise time to bolometric maximum of 19 days, this simple relation gives a total luminosity at maximum light of

$$L_{\text{max}} = 2.0 \times 10^{43} \left(\frac{M_{\text{Ni}}}{M_{\odot}} \right) \text{ erg s}^{-1}. \quad (1)$$

To account for flux outside the optical and near-IR passbands a 10% correction is added to each ^{56}Ni mass estimate obtained from Eq. (1).

Recently, we conducted an investigation (Blinnikov et al. 2006) of Arnett's rule using synthetic light curves computed using the 1-D hydro code STELLA (Sorokina & Blinnikov 2003). This showed that with the UVOIR light curve and this 10% correction, Arnett's rule estimates the ^{56}Ni yield accurately to within $\lesssim 0.05 M_{\odot}$.

4. Results

Armed with our two methods we proceed to estimate the ^{56}Ni mass for seventeen SNe Ia. Figure 2 contains the ^{56}Ni mass determined from the synthetic spectral analysis of the nebular spectra plotted vs. the ^{56}Ni mass determined from the UVOIR light curves. These values are listed in Table 2. Because we compare estimates of the ^{56}Ni mass derived from two independent methods, our results are not affected by the uncertainties associated with the adopted reddening and distance values. We have therefore not included error bars arising from the uncertainty in these quantities. Including the uncertainties in distance and extinction for each event can lead to an

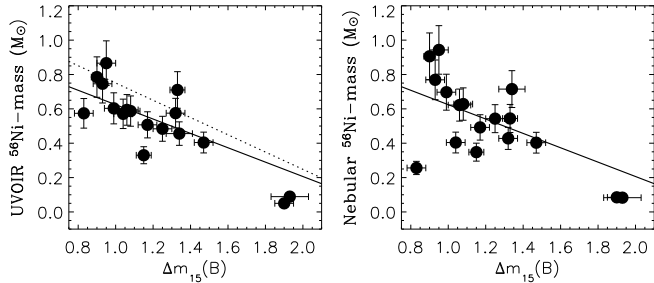


Figure 3 ^{56}Ni mass derived from the UVOIR light curve method (*left*) and the nebular spectrum fitting method (*right*) vs. $\Delta m_{15}(B)$. Solid line in both panels corresponds to the Phillips $M_B - \Delta m_{15}(B)$ relation (Phillips et al. 1999). Dotted lines in the left panel corresponds to the Phillips $M_B - \Delta m_{15}(B)$ relation when the adopted bolometric correction of -0.28 is changed to -0.48 .

uncertainty in the absolute value of each ^{56}Ni mass estimate ranging from ~ 0.05 to $\sim 0.35 M_{\odot}$ (Stritzinger et al. 2006). Instead, plotted in Fig. 2 are offsets from the line with a slope of one. These correspond to 10% (dashed lines) and 20% (dotted lines) respectively. From Fig. 2 it is evident that eleven of the seventeen SNe Ia have ^{56}Ni masses that agree with each other to within 10%, four to within 20%, and only two differ by more than 20%.

In order to assess the intrinsic uncertainty of the spectral synthesis method we varied the size of the error bars on the ^{56}Ni mass estimates and computed the reduced χ^2 . It is found that an uncertainty of 20% clearly overestimates the true random uncertainty while 10% gives a reduced $\chi^2 = 4.0$. We find that an uncertainty between 15% and 20% gives reasonable reduced χ^2 values. For error bars that are 15% of the ^{56}Ni mass estimates we obtain a reduced $\chi^2 = 1.8$. Furthermore if we include a $3\text{-}\sigma$ clipping algorithm, which excludes one event (in this cases SN 1995al) we obtain a reduced $\chi^2 = 1.16$. Clearly the error bar for SN 1995al should be larger than 15%. Moreover, events with poor quality data such as SN 1989B, which has two low signal-to-noise spectra and suffers from high values of extinction may also have an uncertainty larger than 15%. Nevertheless in the following we conclude that an average 15% uncertainty for the error bars is reasonable for the adopted uncertainties in the values of the ^{56}Ni mass estimates from the spectral synthesis method determined with good quality data. As discussed above the ^{56}Ni mass estimates determined via the UVOIR light curve and Arnett’s rule are accurate to within $\sim 10\%$. To be conservative we also adopt a 15% uncertainty for this method.

In Fig. 3 the ^{56}Ni mass derived for each event via both methods is plotted vs. $\Delta m_{15}(B)$. The solid line in both panels corresponds to the $M_B - \Delta m_{15}(B)$ relation given in Phillips

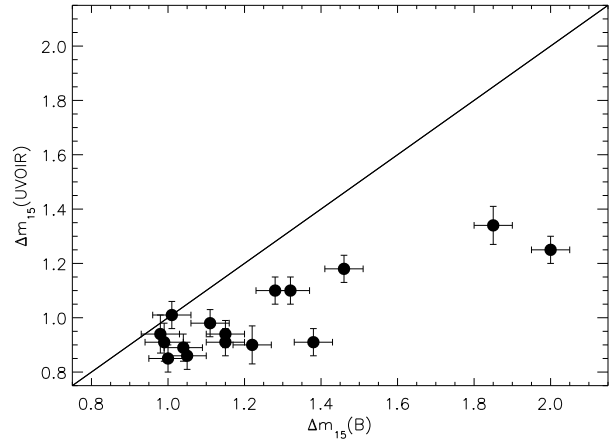


Figure 4 $\Delta m_{15}(UVOIR)$ vs. $\Delta m_{15}(B)$. Solid line has a slope of one. We assume a $\Delta m_{15}(UVOIR)$ uncertainty of 0.05 for each event except those that have a U -band correction. In these cases the uncertainty was increased to 0.07.

et al. (1999, see their Table 3). To convert M_B to a UVOIR luminosity we used the bolometric correction (BC) given by Branch (1992) of -0.28 , and then Eq. 1 to convert luminosity to a ^{56}Ni mass. To illustrate the effect of the adopted BC upon the Phillips relation we have included in the left panel of Fig. 3 (dotted line) the $M_B - \Delta m_{15}(B)$ relation if the BC is decreased to a rather conservative value of -0.42 . As shown in Fig. 3 this leads to a steepening of the Phillips relation. Clearly the ^{56}Ni mass estimates from both methods are correlated to $\Delta m_{15}(B)$. Moreover, this correlation is in excellent agreement with the Phillips $M_B - \Delta m_{15}(B)$ relation. Note that a least squares fit computed from the data gives a line that is very similar to the Phillips relation line. In both cases the least squares line is only slightly steeper.

We found no correlation between ^{56}Ni mass and $\Delta m_{15}(UVOIR)$ for events with $\Delta m_{15}(UVOIR) \leq 1.1$. This motivated us to plot in Fig. 4 $\Delta m_{15}(UVOIR)$ vs. $\Delta m_{15}(B)$.² The solid line corresponds to a slope of one. For all events $\Delta m_{15}(UVOIR)$ is less than $\Delta m_{15}(B)$ except for SN 2000cx which has identical values for both parameters. Evidently $\Delta m_{15}(UVOIR)$ is correlated with $\Delta m_{15}(B)$. Note there are events with similar values of $\Delta m_{15}(UVOIR)$ that show a scatter in $\Delta m_{15}(B)$ of ~ 0.4 mag. Finally, the fact that the estimates of $\Delta m_{15}(B)$ and $\Delta m_{15}(UVOIR)$ are identical for SN 2000cx is most likely due to its asymmetric rise (and fall) to (from) maximum light (see Li et al. 2001).

5. Discussion

The agreement between the ^{56}Ni mass estimates shown in Fig. 2 is very encouraging. We emphasize the point that these two methods are completely independent and use drastically different observational data. The ability to accurately probe the

² By plotting the decline rate parameters rather than a parameter(s) set by an absolute flux scale, we bypass the effects associated with the uncertainty in the adopted distance.

explosion mechanism with one spectrum taken more than 100 days past the explosion reveals the power of the spectral synthesis method.

The range of a factor of ten in the amount of synthesized ^{56}Ni , as indicated by the spectral synthesis method, is consistent with results obtained from previous studies of UVOIR light curves (Suntzeff 1996; Cappellaro et al. 1997; Contardo et al. 2000; Strolger et al. 2002; Suntzeff 2003; Stritzinger et al. 2006). The observed range in ^{56}Ni mass is difficult to reconcile with the current SN Ia paradigm (Nomoto, Thielemann, & Yokoi 1984; Woosley & Weaver 1986; Hillebrandt & Niemeyer 2000), i.e. the thermonuclear disruption of a Chandrasekhar-size white dwarf. This has led to the introduction of the so called delayed detonation model (Khokhlov 1991; Woosley 1990; Woosley & Weaver 1994; Höflich & Khokhlov 1996), and most recently more exotic explosion mechanisms (Bravo & García-Senz 2006). An alternative to the Chandrasekhar mass model that addresses the observed diversity of SNe Ia properties is a variable progenitor mass. There is mounting observational evidence that sub-Chandrasekhar mass white dwarfs are a plausible candidate for the less luminous events and at least for the sub-luminous SN 1991bg-like variety of SNe Ia (Mazzali et al. 1997; Cappellaro et al. 1997; Stritzinger et al. 2006). Yet another possible progenitor maybe a super-Chandrasekhar mass progenitor (Yoon & Langer 2004, 2005).

Efforts to model the light curves of SNe Ia led to the suggestion that the absolute luminosity at maximum light [hence $\Delta m_{15}(B)$] is a direct consequence of the ^{56}Ni mass (Arnett 1982; Höflich 1996; Cappellaro et al. 1997; Mazzali et al. 2001; Pinto & Eastman 2001; Kasen 2006). The strong correlation shown in Fig. 3 between the ^{56}Ni mass and $\Delta m_{15}(B)$ provides clear observational evidence that supports this hypothesis. This argument is strengthened by the excellent agreement between the Phillips $M_B - \Delta m_{15}(B)$ relation with the results in Fig. 3. With the acquisition of more nebular spectra it should be possible to calibrate the ^{56}Ni mass– M_B relation. With this calibration one could then use a nebular spectrum to (1) determine the distance to a nearby SN Ia, and more importantly (2) address the relationship between the ^{56}Ni mass and the peak absolute magnitudes. We stress that this method is completely independent of the luminosity-decline rate relation, so distances determined through this method are not as susceptible to the secondary parameters that may affect the peak phase light curve (Hamuy et al. 1996; Mazzali et al. 1998; Tripp & Branch 1999; Hatano et al. 2000; Benetti et al. 2004, 2005). The late-time bolometric luminosity, however, may be susceptible to the distribution of isotopes and/or the fraction of positron kinetic energy that is deposited within the ejecta. Nonetheless, by gaining a deeper understanding of how the peak absolute brightness relates to the ^{56}Ni mass we can open a new avenue to understand the explosion mechanism and any possible systematic errors incurred via their relationship.

The scatter seen between $\Delta m_{15}(UVOIR)$ and $\Delta m_{15}(B)$ hints to the complexities associated with the transfer of radiation through an expanding ejecta, and how time-dependent NLTE effects influence the flux evolution of the near-IR light curves. Indeed a comparison between the near-IR light curves

for events with similar values of $\Delta m_{15}(B)$ indicates a diversity in their morphology.

The knowledge afforded through the spectral synthesis method is significant and warrants further efforts on the part of SNe Ia observational programs to obtain well-calibrated nebular spectra.

Acknowledgements. The Dark Cosmology Centre is funded by the Danish National Research Foundation. M.S. and P. M. are grateful to Wolfgang Hillebrandt for his generous hospitality. This work is supported in part by the European Community’s Human Potential Programme under contract HPRN-CT-2002-00303, “The Physics of Type Ia Supernovae”. This research has made use of the NASA/IPAC Extragalactic Database (NED), which is operated by the Jet Propulsion Laboratory, California Institute of Technology, under contract with the National Aeronautics and Space Administration.

References

- Arnett, W. D. 1982, *ApJ*, 253, 785
- Astier, P., Guy, J., Pain, R., et al. 2006, *A&A*, 447, 31
- Axelrod, T. S., 1980, PhD Thesis, Univ. of California, Santa Cruz
- Benetti, S., Meikle, P., Stehle, M., et al. 2004, *MNRAS*, 348, 261
- Benetti, S., Cappellaro, E., Mazzali, P. A., et al. 2005, *ApJ*, 623, 1011
- Blinnikov, S., Röpke, F. K., Sorokina, E. I., et al. 2006, *A&A*, 453, 229
- Branch, D. 1992, *ApJ*, 392, 35
- Branch, D., Dang, L. C., Hall, N., et al. 2006, *PASP*, 118, 560
- Bravo, E., & García-Senz, D. 2006, *ApJ*, 642, L157
- Buta, R., & Turner, A. 1983, *PASP*, 95, 72
- Candia, P., Krisciunas, K., Suntzeff, N. B., et al. 2003, *PASP*, 115, 277
- Cappellaro, E., Mazzali, P. A., Benetti, S., et al. 1997, *A&A*, 329, 203
- Cappellaro, E., Patat, F., Mazzali, P. A., et al. 2001, *ApJ*, 549, L215
- Contardo, G., Leibundgut, B., & Vacca, W. D. 2000, *A&A*, 359, 876
- Filippenko, A. V., Richmond, W., Branch, D., et al. 1992, *AJ*, 104, 1543
- Freedman, W. L., Madore, B. F., Gibson, B. K., et al. 2001, *ApJ*, 553, 47
- Garnavich, P., Bonanos, A., Krisciunas, K., et al. 2004, 613, 1120
- Hamuy, M., Phillips M. M., Suntzeff, N. B., et al. 1996, *AJ*, 112, 2391
- Hatano, K., Branch, D., Lentz, E., et al. 2000, *ApJ*, 543, L49
- Hillebrandt, W., & Niemeyer, J. C. 2000, *ARA&A*, 38, 191
- Höflich, P., Khokhlov, A., Wheeler, C., et al. 1996, *ApJ*, 472, L81
- Höflich, P., & Khokhlov A. 1996, *ApJ*, 457, 500
- Jha, S. 2002, Harvard University Dissertation
- Jha, S., Branch, D., Chornock, R., et al. 2006, *AJ*, 132, 189
- Kasen, D. 2006, *ApJ*, in press
- Khokhlov, A. M. 1991, *A&A*, 245, 114
- Kotak, R., Meikle, W. P. S., Pignata, G., et al. 2005, *A&A*, 436, 1021
- Kozma, C., Fransson, C., Hillebrandt, W., et al. 2005, *A&A*, 437, 983
- Kraan-Korteweg, R. C. 1986, *A&AS*, 66, 255
- Krisciunas, K., Suntzeff, N. B., Candia, P., et al. 2003, *AJ*, 125, 166
- Li, W., Filippenko, A. V., Gates, E., et al. 2001, *PASP*, 113, 1178
- Lira, P., Suntzeff, N. B., Phillips, M. M., et al. 1998, *AJ*, 115, 234
- Leibundgut, B. 2001, *A&A Rev.*, 39, 67
- Leibundgut, B., Kirshner, R., Phillips, M., et al. 1993, *AJ*, 105, 301
- Mattila, S., Lundqvist, P., Sollerman, J., et al. 2005, *A&A*, 443, 649
- Mazzali, P. A., Chugai, N., Turatto, M., et al. 1997, *MNRAS*, 284, 151
- Mazzali, P. A., Cappellaro, E., Danziger, I. J., et al. 1998, *ApJ*, 499, L49
- Mazzali, P. A., Nomoto, K., Cappellaro, E., et al. 2001, *ApJ*, 547, 988
- Mazzali, P. A. 2006, in preparation
- Meikle, W. P. S. (private communication)
- Meikle, W. P. S., Cumming R. J., Geballe T. R., et al. 1996, *MNRAS*, 281, 263
- Nomoto, K., Thielemann, F.-K., & Yokoi, K. 1984, *ApJS*, 286, 644
- Patat, F., Benetti, S., Cappellaro, E., et al. 1996, *MNRAS*, 278, 111
- Phillips, M. M., Lira, P., Suntzeff, N. B., et al. 1999, *AJ*, 118, 1766
- Pignata, G., Patat, F., Benetti, S., et al. 2004, *MNRAS*, 355, 178
- Pinto, P. A., & Eastman, R. G. 2001, *New Astronomy*, 6, 307
- Richmond, M. W., Treffers, R. R., Filippenko, A. V., et al. 1995, *AJ*, 109, 2121
- Riess, A. G., Kirshner, R. P., Schmidt, B. P., et al. 1999a, *AJ*, 117, 707
- Riess, A. G., Strolger, L. G., Tonry, J., et al. 2004, *ApJ*, 607, 665
- Ruiz-Lapuente, P., & Lucy, L.B. 1992, *ApJ*, 400, 127
- Salvo, M. E., Cappellaro, E., Mazzali, P. A., et al. 2001, *MNRAS*, 321, 254
- Smith, C. (private communication)
- Sollerman, J., Lindahl, J., Kozma, C., et al. 2004, *A&A*, 428, 555
- Spyromilio, J., Gilmozzi, R., Sollerman, J., et al. 2004, *A&A*, 426, 547
- Sorokina, E., & Blinnikov, S. 2003, in: *From Twilight to Highlight, The Physics of Supernovae*, ed. W. Hillebrandt & B. Leibundgut, Heidelberg:Springer, 268
- Stanishev, V., et al. 2006, *A&A*, submitted
- Stehle, M., Mazzali, P. A., Benetti, S., Hillebrandt, W. 2005, *MNRAS*, 360, 1231
- Strolger, L. G., Smith, R. C., Suntzeff, N. B., et al. 2002, *AJ*, 124, 2905
- Stritzinger, M. D., & Leibundgut, B. 2005, *A&A*, 431, 423
- Stritzinger, M. D., Leibundgut, B., Walch, S., Contardo, G. 2006, *A&A*, 450, 24
- Suntzeff, N. B. 1996, in: *IAU Colloquium 145, Supernovae and Supernova Remnants*, ed. R. McCray, & Z. Wang, Cambridge University Press, Cambridge, 41
- Suntzeff, N. B. 2003, in: *From Twilight to Highlight, The Physics of Supernovae*, ed. W. Hillebrandt & B. Leibundgut, Heidelberg:Springer, 183
- Suntzeff, N. B., Phillips, M., Covarrubias, R., et al. 1999, *AJ*, 117, 1175
- Tripp, R., & Branch, D. 1999, *ApJ*, 525, 209
- Turatto, M., Benetti, S., Cappellaro, E., et al. 1996, *MNRAS*, 283, 1
- Wells, L., Phillips, M. M., Suntzeff, N. B., et al. 1994, *AJ*, 108, 2233

- Woosley, S. W. 1990, in: *Supernovae*, eds, A. Petschek, Berlin:Springer-Verlag, 182
- Woosley, S. W., & Weaver, T. A. 1986, *ARA&A*, 24, 205
- Woosley, S. W., & Weaver, T. A. 1994, in: *Supernovae, Les Houches Session LIV*, eds, J. Audouze, S. Bludman, R. Mochovitch, J. Zinn-Justin, Amsterdam:Elsevier, 63
- Yoon, S.-C., & Langer, N. 2004, *A&A*, 419, 623
- Yoon, S.-C., & Langer, N. 2005, *A&A*, 435, 967

Table 1. The SNe Ia sample

| SN | Ref. ^a | N ^b | Filters | Ref. ^c | $E(B - V)_{\text{tot}}^d$ | μ^e | $\Delta m_{15}(B)^f$ |
|--------|-------------------|----------------|--------------|--------------------|---------------------------|---------|----------------------|
| 1989B | W94 | 2 | <i>BVRI</i> | W94 | 0.370 | 29.86 | 1.34±0.07 |
| 1990N | AA | 1 | <i>UBVRI</i> | L98 | 0.020 | 31.90 | 1.08±0.05 |
| 1991T | AA | 1 | <i>UBVRI</i> | L98 | 0.140 | 30.74 | 0.95±0.05 |
| 1991bg | T96 | 3 | <i>BVRI</i> | F92, L93, T96 | 0.060 | 31.13 | 1.93±0.10 |
| 1992A | M97 | 1 | <i>UBVRI</i> | S96 | 0.020 | 31.41 | 1.47±0.05 |
| 1994D | M97 | 5 | <i>UBVRI</i> | R95, P96, M96, S00 | 0.040 | 30.90 | 1.32±0.05 |
| 1994ae | M97 | 1 | <i>BVRI</i> | R99 | 0.150 | 32.22 | 0.90±0.03 |
| 1995D | M97 | 2 | <i>BVRI</i> | R99 | 0.090 | 32.43 | 0.99±0.05 |
| 1995al | AA | 1 | <i>BVRI</i> | R99 | 0.160 | 32.00 | 0.83±0.05 |
| 1996X | S01 | 1 | <i>UBVRI</i> | R99,S01 | 0.060 | 32.02 | 1.25±0.05 |
| 1998bu | C01 | 3 | <i>UBVRI</i> | J02, S99 | 0.350 | 29.97 | 1.04±0.05 |
| 1999by | J06 | 1 | <i>UBVRI</i> | G04 | 0.000 | 30.03 | 1.90±0.05 |
| 2000cx | S04 | 1 | <i>UBVRI</i> | J02, Li01, C03 | 0.080 | 32.64 | 0.93±0.05 |
| 2001el | M05 | 1 | <i>UBVRI</i> | K03 | 0.240 | 30.55 | 1.15±0.04 |
| 2002bo | B04 | 2 | <i>UBVRI</i> | B04 | 0.380 | 31.67 | 1.17±0.05 |
| 2002er | K05 | 1 | <i>UBVRI</i> | P04 | 0.360 | 32.90 | 1.33±0.04 |
| 2003du | VS06 | 1 | <i>UBVRI</i> | VS06 | 0.000 | 32.75 | 1.06±0.06 |

^aReference to the nebular spectrum.

^bN is the number of nebular spectra used to estimate the ^{56}Ni mass.

^cReference(s) to the photometric data.

^dReddening values are from the references quoted in column 5 or are at least consistent with their estimate.

^eCepheid distances for SNe 1989B, 1991T, and 1998bu taken from Freedman et al. (2001) ($H_0 = 72 \text{ km s}^{-1} \text{ Mpc}^{-1}$). For the remaining events, the relative distances to Virgo are taken from Kraan-Korteweg (1986) adopting a Virgo distance of 15.3 Mpc or distances from the Hubble flow.

^fIf available, values of $\Delta m_{15}(B)$ were taken from Benetti et al. (2005), otherwise they were taken from Phillips et al. (1999) or from the literature.

References. — (AA) Asiago SN archive; (B04) Benetti et al. 2004; (C01) Cappellaro et al. 2001; (C03) Candia et al. 2003; (F92) Filippenko et al. 1992; (G04) Garnavich et al. 2004; (J02) Jha 2002; (J06) Jha et al. 2006; (K05) Kotak et al. 2005; (K03) Krisciunas et al. 2003; (L93) Leibundgut et al. 1993; (L98) Lira et al. 1998; (L01) Li et al. 2001; (M96) Meikle et al. 1996; (M97) Mazzali et al. 1997; (M05) Mattila et al. 2005; (P96) Patat et al. 1996; (P04) Pignata et al. 2004; (R95) Richmond et al. 1995; (R99) Riess et al. 1999a; (S00) Smith, priv. comm.; (S01) Salvo et al. 2001; (S04) Sollerman et al. 2004; (S96) Suntzeff 1996; (S99) Suntzeff et al. 1999; (T96) Turatto et al. 1996; (VS06) Stanishev et al. 2006; (W94) Wells et al. 1994.

Table 2. Derived SNe Ia parameters

| $\Delta m_{15}(UVOIR)$ | $^{56}\text{Ni}(UVOIR)$ (M_{\odot}) | $^{56}\text{Ni}(\text{nebular})$ (M_{\odot}) | SN |
|------------------------|--|---|--------|
| 0.85 | 0.87 | 0.94 | 1991T |
| 0.85 | 0.57 | 0.26 | 1995al |
| 0.86 | 0.59 | 0.63 | 1990N |
| 0.89 | 0.59 | 0.62 | 2003du |
| 0.90 | 0.46 | 0.72 | 1989B |
| 0.91 | 0.40 | 0.40 | 1992A |
| 0.91 | 0.33 | 0.35 | 2001el |
| 0.94 | 0.60 | 0.70 | 1995D |
| 0.94 | 0.51 | 0.49 | 2002bo |
| 0.95 | 0.79 | 0.91 | 1994ae |
| 0.98 | 0.57 | 0.40 | 1998bu |
| 1.02 | 0.75 | 0.77 | 2000cx |
| 1.10 | 0.48 | 0.54 | 1996X |
| 1.10 | 0.71 | 0.54 | 2002er |
| 1.18 | 0.58 | 0.43 | 1994D |
| 1.25 | 0.05 | 0.09 | 1999by |
| 1.42 | 0.09 | 0.08 | 1991bg |